

SPATIAL RESOLUTION AND CLOUD OPTICAL THICKNESS RETRIEVALS

Rand E. Feind, Sundar A. Christopher and Ronald M. Welch

Institute of Atmospheric Sciences
South Dakota School of Mines and Technology
501 E. St. Joseph Street
Rapid City, South Dakota 57701-3995

1. INTRODUCTION

In this study, we investigate the impact of sensor spatial resolution and accurate cloud pixel identification on cloud property retrievals. Twelve fair weather cumulus (FWC) scenes of high spectral and spatial resolution Airborne Visible and Infrared Imaging Spectrometer (AVIRIS) data are analyzed. A variation of the 3-band ratio technique of Gao and Goetz is used to discriminate clouds from the background, and then a discrete ordinate radiative transfer model is used to obtain optical thickness of cloudy regions for each scene. To study the effect of spatial resolution upon retrieved optical thickness, the 20 m AVIRIS data was spatially degraded to spatial resolutions ranging from 40 to 960 m. Cloud area, scene average optical thickness, and distribution of retrieved optical thickness are determined at each spatial resolution. Finally, a comparison between the 3-band ratio technique and monospectral reflectance thresholding, using 20 m spatial resolution data, is presented.

2. METHODOLOGY

Gao and Goetz (1991) developed a method that takes advantage of high spectral resolution imagery and greatly facilitates the ability to distinguish between cloud and background pixels. The method for cloud pixel identification employs a 3-band ratio and is computed as the sum of the radiance from the imagery at 0.94 and 1.14 μm divided by twice the radiance at 1.04 μm . In the 3-band ratio imagery, the land background is somewhat homogenized, while the clouds retain their features. Identification of cloud pixels at a non-absorbing wavelength (such as 0.74 μm) is a three-step process: 1) the selection of a threshold for water/shadow background areas; 2) the selection of a 3-band ratio threshold in the 3-band ratio image; and 3) the application of a cloud pixel mask (determined by the first two steps) to the appropriate wavelength imagery.

Each cloud pixel in the masked 0.74 μm radiance image is assigned one of 18 different optical thickness values based on the results of a discrete ordinate radiative transfer model (Stamnes *et al.*, 1988). Lower spatial resolution instrument imagery is emulated through spatial averaging of the 20 m AVIRIS data. Three-band ratio masks are obtained at lower spatial resolutions and are applied to like imagery at 0.74 μm . Estimates of average optical thickness and cloud area are then obtained at all spatial resolutions.

3. RESULTS

Figure 1 shows the percent change in cloud area as a function of spatial resolution for the 12 images used in this investigation. There is a large dependence upon spatial resolution. Of interest is the fact that there is a great deal of scatter in the

results, especially as spatial resolution is degraded, suggesting no precise way to correct for these errors. The effect of spatial resolution upon cloud average optical thickness retrieval is shown in Fig. 2. The results are expressed in terms of the percent change in average cloud optical thickness, relative to 20 m resolution imagery, as a function of spatial resolution. Figure 2 shows that cloud optical thickness decreases monotonically with decreasing spatial resolution. Figure 3 shows the product of optical thickness and cloud area as a function of spatial resolution. One would expect the curves to be relatively flat and they are relatively flat out to spatial resolutions on the order of 300 m; however, the curves still decrease with decreasing spatial resolution.

Histograms of cloud optical thickness for one of the analyzed scenes appear in Fig. 4. It shows that the distribution of cloud optical thickness changes with spatial resolution; however, it does not change in a predictable manner. Perhaps the most notable trend is that the frequency of occurrence of the largest values of optical thickness decreases with decreasing spatial resolution.

We examine the consequences upon cloud optical depth retrieval when applying simple reflectance thresholds. First we compute the monospectral ($0.74 \mu\text{m}$) reflectance threshold which produces the same cloud area as obtained by the 3-band ratio technique. The results for the 12 scenes, in % above background albedo, are as follows: A - 3.2, B - 5.5, C - 4.1, D - 4.3, E - 3.2, F - 4.5, G - 5.8, H - 3.1, I - 8.4, J - 8.0, K - 3.7, L - 5.0. These results indicate that the required reflectance threshold is scene dependent. Shown in Fig. 4 is the impact of assigning a monospectral reflectance for optical thickness retrievals. The optical thickness histogram is shown for both the 3-band ratio technique and for the aforementioned monospectral reflectance thresholds. Differences in the optical thickness retrievals are found in the optically thinner areas of the cloud, $t < 4$. These differences are found at all spatial resolutions. In addition, the distribution of gray levels for cloud edges is determined by histogramming the edge maps of the masked $0.74 \mu\text{m}$ images. Results (not presented herein) show that the distributions are relatively broad (approximately 10% of the available scene reflectance), indicating that a single monospectral reflectance threshold is inadequate for identifying cloud edge pixels.

4. CONCLUSIONS

The present results demonstrate that both spatial and spectral resolution significantly impact our ability to retrieve cloud optical thickness properties accurately. Decreasing spatial resolution from 20 m to 960 m dramatically affects estimates of cloud area, average optical thickness, and the distribution of retrieved optical thickness. The change in these estimates with change in spatial resolution is scene dependent. It is shown that some of the error in estimates for average optical thickness is due to the error in estimates of cloud area; however, when the effect of increasing cloud area with decreasing spatial resolution is removed, average optical thickness still decreases with decreasing spatial resolution. It is also shown that the use of a single, monospectral reflectance threshold is inadequate for identifying cloud pixels in FWC scenes, pointing to the necessity of using high spectral resolution data, combined with appropriate processing algorithms. In a monospectral image, not only is the optimum threshold (with respect to background albedo) scene dependent, but also the edge around a single cloud cannot be located by using a single threshold. Although cloud edges are, in general, optically thin, they can significantly impact estimates of average optical thickness. These results have potentially important consequences because most commonly used cloud retrieval algorithms apply a single reflectance threshold.

As a caveat, it should be noted that the results reported here are only for FWC over land, perhaps one of the most difficult cloud types to retrieve accurately using satellite imagery. Obviously, stratiform cloud properties are retrieved with far greater certainty. Nevertheless, even a cursory examination of a GOES image demonstrates that a large fraction of cloudiness is inhomogeneous. Problems with correct cloud edge identification and spatial resolution can be expected for all inhomogeneous cloud fields.

Acknowledgments. This research is supported by the NASA EOS Program for ASTER and HIRIS science algorithm development under Contracts NAS5-30958, NAS5-30768, and NAS5-31718. Appreciation is extended to B.K. Gao and K-S Kuo for their comments and discussion and to J. Robinson for typing this paper.

REFERENCES

Gao, B. C. and Goetz, A. F. H., "Cloud area determination from AVIRIS data using water vapor channels near 1 μm ," *J. Geophys. Res.* vol. 96, no. D2, pp. 2857-2864, 1991.

Stamnes, K., Tsay, S. C., Wiscombe, W., and Jayaweera, K., "A numerically stable algorithm for discrete-ordinate-method radiative transfer in multiple scattering and emitting layered media," *Appl. Opt.*, vol. 17, pp. 2502-2509, 1988.

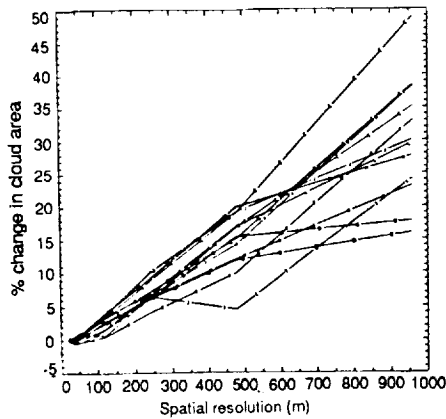


Fig. 1: Percent change in cloud cover, referenced to 20 m resolution, as a function of spatial resolution for the 12 scenes.

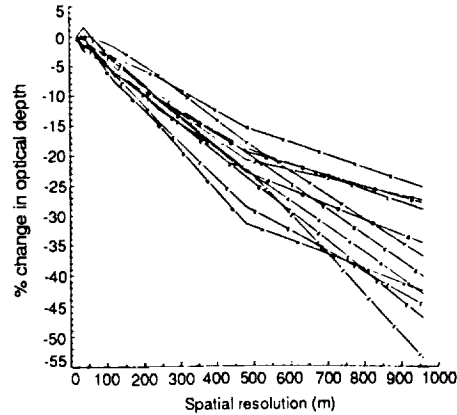


Fig. 2: Percent change in cloud average optical thickness, referenced to 20 m resolution, as a function of spatial resolution.

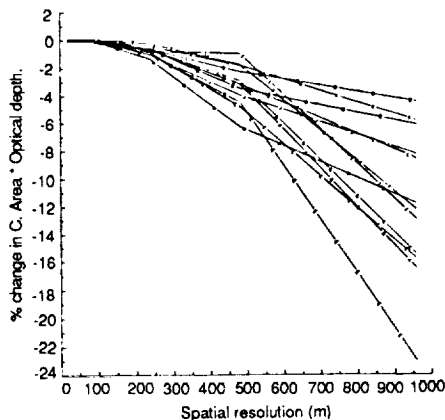


Fig. 3: Percent change in the product of cloud area and cloud optical thickness, referenced to 20 m resolution, as a function of spatial resolution.

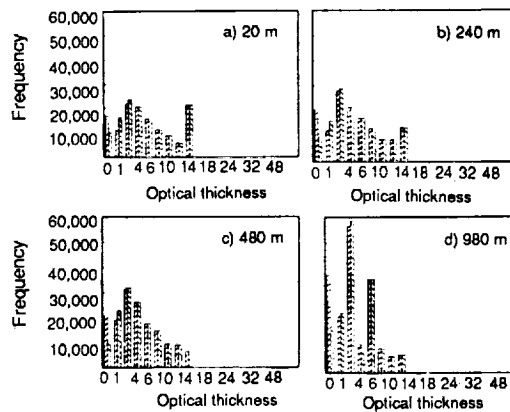


Fig. 4: Frequency distribution of cloud optical thickness for spatial resolutions of A) 20 m; B) 240 m; C) 480 m; and D) 960 m. \square denote the 3-band ratio results, and the \square denote results for a reflectance threshold of 4.95 above background.